# Characterization of $Pt_n$ ($n$ = 2–12) clusters through global reactivity descriptors and vibrational spectroscopy, a theoretical study

C.L. Heredia [a,b], V. Ferraresi-Curotto [a,c], M.B. López [a,*]

[a] CIFTA, Centro de Investigaciones Fisicoquímicas, Teóricas y Aplicadas, Facultad de Ciencias Exactas y Naturales, Universidad Nacional de Catamarca, Av. Belgrano 300, 4700 Catamarca, Argentina
[b] INIQUI, Instituto de Investigación para la Industria Química (CONICET), Facultad de Ciencias Exactas, Universidad Nacional de Salta, Av. Bolivia 5150, A4408FVY Salta, Argentina
[c] CEQUINOR, Centro de Química Inorgánica (CONICET), Facultad de Ciencias Exactas, Universidad Nacional de La Plata CC 962, B1900AVV La Plata, Argentina

## ARTICLE INFO

## ABSTRACT

Geometric, magnetic and electronic features, vibrational frequencies and global reactivity descriptors of $Pt_n$ ($n$ = 1–12) were studied in the present work within the framework of the density functional theory. Structures for $n$ = 7, 10, 11 and 12 have not been reported before, in other cases agreement exists with results reported by other authors, as are the data obtained through vibrational spectroscopy calculations. Results obtained from global reactivity descriptors such as chemical potential, chemical hardness and electrophilicity index, indicate that platinum clusters up to twelve atoms tend to increase their reactivity with size.

## 1. Introduction

The interest on the area of atomic clusters has rapidly grown within the last three decades not only because of their unique size-dependent structures and different properties from those of the bulk, but also due to their central position, on the one hand, among molecules, and on the other, among condensed matter [1]. In particular, transition metal clusters have been studied for its potential use as catalysers and in the production of electronic nanodevices. Among these, Pt is one of the ingredients in the catalyst used in car catalytic converters to reduce toxic pollutants, such as CO, NOx, and hydrocarbons, and it is also an important material for the hydrogenation in heterogeneous catalysis [2].

Experimental studies on small free Pt clusters are scarce. Taylor and co-workers [3] used resonant two-photon ionization spectroscopy of jet-cooled $Pt_2$ to find numerous platinum vibrational bands. Jansson and Scullman [4] measured the vibrational spectrum of a $Pt_2$ in an Ar matrix. Gupta and co-workers [5] were successful in detecting $Pt_2$ over the temperature range 2259–2739 K. Airola and Morse [6] were able to measure the resolved rotational spectrum of the $Pt_2$. They determined very precise values for bond energy, bond length, and ground-state vibrational frequency. Lineberger and co-workers investigated the electronic spectra of small platinum and palladium clusters by the negative ion photodetachment spectroscopic method, up to a size of three atoms [7,8] and Eberhardt and co-workers obtained the valence and core-level photoemission spectra of mass selected monodispersed $Pt_n$ ($n$ = 1–6) clusters [9].

Regarding theoretical studies, ab initio calculations on the Pt clusters are also scarce, especially for $Pt_n$ with $n$ greater than 10. Ellis et al. [10] studied the $Pt_4$ cluster using an ab initio generalized valence bond method within the relativistic effective core potential and a double-zeta basis set. Complete active space self consistent-field (CASSCF) calculations followed by the first-order configuration interaction (FOCI) computations were performed by Balasubramanian [11] on the $Pt_2$ and by Dai and Balasubramanian [12] on the $Pt_4$ clusters to study their electronic structures. Yang and co-workers [13] applied the non-self consistent Harris functional version [14] of the local density approximation (LDA) within the density functional theory (DFT) to obtain minimum energy structures of the $Pt_n$ clusters for $n$ = 2–6. Fortunelli [15] has performed DFT calculations on small $Pt_n$ clusters ($n$ = 1–4) using Amsterdam Density Functional (ADF) program [16]. Apra and Fortunelli [17] carried out DFT calculations on $Pt_{13}$ and $Pt_{55}$ cuboctahedral clusters using DFT module of the NW-Chem computational chemistry package [18]. The structural, energetic, electronic, and magnetic properties of platinum clusters of up to 55 atoms were studied by Xiao and Wang [19] using DFT with a plane wave basis set implemented in the Vienna ab initio simulation package (VASP). The spin–orbit coupling and its impact in determining the structures of platinum nanoclusters ($Pt_n$, $n$ = 2–5) was studied by Huda and collaborators [20] using the projected

* Corresponding author. Tel./fax: +54 3833 420900.
*E-mail address:* mblopez@fcasuser.unca.edu.ar (M.B. López).

augmented wave method (PAW) within the VASP. Nie and collaborators [21] analyzed the structural evolution of small minimum energy platinum clusters, ($Pt_n$, $n = 2$–15) using DFT within the generalized gradient approximation (GGA) with Perdew–Wang exchange–correlation functional (PW91) as implemented in DMol3 package. Bhattacharyya and Majumder [22] studied the growth pattern and bonding trends in $Pt_n$ ($n = 2$–13) clusters using DFT with PAW method and plane wave basis set as implemented in VASP code. Kumar and Kawazoe [23] applied ultrasoft pseudopotential and PAW methods to study the evolution of atomic and electronic structure of $Pt_n$ clusters in a wide range of sizes starting from two atoms to nanoparticles having a diameter of about 3 nm. Finally, Sebetci [24] performed full-relativistic DFT calculations to study the geometries and binding energies of different isomers of free platinum clusters $Pt_n$ ($n = 4$–6) within the spin multiplicities from singlet to nonet. Another work performed by Sebetci [25] shows a DFT study of hydrogen–platinum clusters, $Pt_nH_m$ ($n = 1$–5, $m = 0$–2), in which he analyses structures of pure platinum. All theoretical studies mentioned above analyzed the evolution of structural and electronic properties of $Pt_n$ series. Close attention was paid to the tendency to form plane or three-dimensional structures and their impact on electronic properties.

The aim of the present work is the characterization of neutral platinum clusters in terms of reactivity descriptors. These reactivity descriptors have already been successfully used in clusters [26], in different kinds of molecular structures and in chemical reactions [27]. DFT gave a new impact to the theory of reactivity. Parr and Pearson [28] derived the concept of reactivity descriptors like chemical potential ($\boldsymbol{\mu}$), electronegativity ($\boldsymbol{\chi}$), chemical hardness ($\boldsymbol{\eta}$) and softness ($S = 1/\boldsymbol{\eta}$). These quantities, known as global reactivity indexes, served to apply the hard-soft acid–base (HSAB) principle by Pearson [29]. Shortly after the definition of hardness, Parr and Yang [30] rationalized the frontier orbital theory of Fukui from DFT. They introduced local reactivity indexes such as the condensed Fukui function, local softness and electrophilicity, to characterize specific sites within a molecule. In the present study we focus our attention on the study of global reactivity indexes.

In order to assess the use of the DFT-concepts and principles just mentioned for the solid state system characterization, we perform a study of the structural, magnetic, energetic, and electronic properties of $Pt_n$ ($n = 2$–12), with special attention on the performance of the different reactivity descriptors so as to get information on the behavior of platinum clusters. In addition, the vibrational frequencies and infrared intensities on ground-state structures are also reported.

## 2. Computational methods

DFT computations were carried out with Gaussian 03 suite of programmes [31]. B3PW91 hybrid functional was used, which combines Becke's three-parameters exchange functional (B3) [32], with Perdew–Wang correlation functional (PW91) [33,34]; with LANL2DZ pseudopotential, which describes 1s to 4f core electrons and leaves 18 valence electrons explicit for computations [35], corresponding to $5s^2 5p^6 5d^9 6s^1$ electronic configuration.

Geometry optimizations on neutral and ionic platinum isomers up to 12 atoms are performed without symmetry constraints. Moreover, the total electronic energy is minimized respecting to the electron spin multiplicity. For a given starting geometry several optimizations are accomplished with different values of the electron spin multiplicity, which is kept fixed during the calculations. The hessian matrix of the total electronic energy respecting to the nuclear coordinates is diagonalized to verify whether the optimized geometries are true minima or saddle points on the potential energy surface of the clusters. As a consequence, vibrational frequencies and infrared intensities are obtained. As a

stability criterion, the absolute value of the binding energy per atom (BE/at) was used, obtained in the following way:

$$\text{BE/at} = \frac{[n\text{E(Pt)} - \text{E}(Pt_n)]}{n} \quad (n = 2, 3 \ldots) \tag{1}$$

where E(Pt) stands for the total energy of platinum atom, $\text{E}(Pt_n)$ corresponds to the total energy of cluster $Pt_n$ and $n$ is the total number of atoms. Energies correspond to the ground state of the species.

Vertical ionization potentials (IP) and electron affinities (EA) are calculated as the total energy difference of neutral and charged clusters according to [36], as:

$$\text{IP}(Pt_n) = \text{E}(Pt_n^+) - \text{E}(Pt_n) \tag{2}$$

and

$$\text{EA}(Pt_n) = \text{E}(Pt_n) - \text{E}(Pt_n^-) \tag{3}$$

where $\text{E}(Pt_n)$, $\text{E}(Pt_n^+)$, $\text{E}(Pt_n^-)$ and $n$ refer to the total energy of the neutral cluster, total energy of the cationic cluster, total energy of the anionic cluster and the total number of atoms, respectively.

Each system's electronic chemical potential ($\boldsymbol{\mu}$) and chemical hardness ($\boldsymbol{\eta}$) were next computed from the ionization potentials and electron affinities based upon the finite difference approximation [37]:

$$\boldsymbol{\mu} = -\frac{1}{2}(\text{IP} + \text{EA}) \tag{4}$$

and

$$\boldsymbol{\eta} = -\frac{1}{2}(\text{IP} - \text{EA}) \tag{5}$$

In particular, $\boldsymbol{\mu}$ characterizes the escaping tendency of electrons from the equilibrium system while $\boldsymbol{\eta}$ can be seen as a resistance to charge transfer. These two entities, as IP and EA, are global properties of the systems researched. The global electrophilicity index ($\boldsymbol{\omega}$), which is derived from the chemical potential and hardness and measures the stabilization in energy when a system gets an additional electronic charge from the environment, was defined by Parr as [37]:

$$\boldsymbol{\omega} = \frac{\boldsymbol{\mu}^2}{2\eta} \tag{6}$$

Magnetic moments were calculated, in Bohr magneton per atom, as follows,

$$\mu_B/\text{at} = \frac{(m_u - m_d)}{n} \tag{7}$$

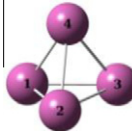where $m_u$ and $m_d$ are electron numbers of different spin states (up, down).
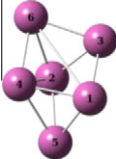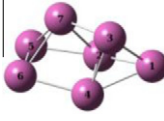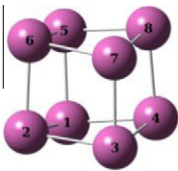
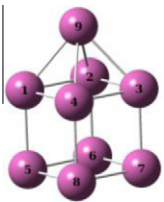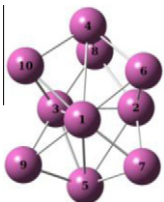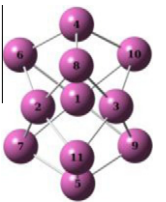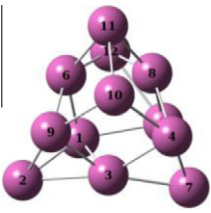## 3. Results and discussion

### 3.1. Structural, magnetic and energetic properties

We have optimized several geometries for $Pt_n$, $n = 2$–12 series starting with non-planar and planar configurations. No negative frequencies are obtained for the clusters; therefore, all clusters are true minima in the potential energy surface. Table 1 depicts the lowest energy structures obtained for the platinum clusters. It is noted that the platinum clusters tend to form three-dimensional structures from the tetramer. These results agree with other theoretical studies [19,22]. The optimized bond length of $Pt_2$ is found to be 2.36 Å in agreement with the experimental value of 2.33 Å [6]. It is also noted that this cluster prefers triplet electronic state.

According to our results $Pt_3$ ground state geometry is an equilateral triangle with Pt–Pt distances of 2.50 Å and characterized

**Table 1**
Properties of the most stable Pt clusters found in the present work. Comparison with experimental results found by other authors is made when available. $\langle R \rangle$ is the average interatomic distance, $\langle CN \rangle$ is the mean coordination number, $m$ is the electron spin multiplicity and $\mu_B$ is the magnetic moment per atom in Bohr magneton.

|  | $Pt_2$ | $Pt_3$ | $Pt_4$ | $Pt_5$ | $Pt_6$ | $Pt_7$ |
|---|---|---|---|---|---|---|
| BE/at | 1.35 | 1.86 | 2.17 | 2.32 | 2.46 | 2.59 |
| $\langle R \rangle$ | 2.36 | 2.50 | 2.61 | 2.79 | 2.61 | 2.74 |
|  | 2.33 [7] | 2.66 [14] |  |  |  |  |
| $\langle CN \rangle$ | 1.0 | 2.0 | 3.0 | 3.20 | 3.00 | 4.66 |
| $m$ | 3 | 1 | 3 | 5 | 7 | 3 |
| $\mu_B$/at | 1.00 | 0.00 | 0.50 | 0.80 | 1.00 | 0.29 |

|  | $Pt_8$ | $Pt_9$ | $Pt_{10}$ | $Pt_{11}$ | $Pt_{12}$ |
|---|---|---|---|---|---|
| BE/at | 2.72 | 2.78 | 2.85 | 2.94 | 2.98 |
| $\langle R \rangle$ | 2.58 | 2.60 | 2.75 | 2.62 | 2.77 |
| $\langle CN \rangle$ | 3.0 | 3.11 | 4.8 | 3.6 | 3.9 |
| $m$ | 9 | 7 | 7 | 7 | 1 |
| $\mu_B$/at | 1.00 | 0.67 | 0.60 | 0.55 | 0.00 |

by a singlet electronic state, in agreement with Bhattacharyya [22]. The Pt–Pt distance for the trimer has been experimentally measured by scanning tunnelling microscopy (STM), resulting in 2.66 Å [38].

Pt$_4$ cluster is the smallest cluster which shows a three-dimensional structural motif. It was found that the tetrahedral geometry is the most stable; with a bond length of 2.61 Å characterized by a triplet electronic state, in agreement with other groups' findings [15,19,21,25]. It is worth saying that other groups report the rhombus as the lowest energy structure [13,22,23].

For Pt$_5$, our results show the distorted squared pyramid geometry as the lowest energy isomer with 2.79 Å average value of interatomic distance and quintet electronic state. It should be pointed out that this structure is 0.004 eV/at more stable than the bipyramid found by other groups [11,13,14].

The most stable structure of the Pt$_6$ cluster is a capped bipyramid with an average bond distance of 2.61 Å and characterized by a septet electronic state. This structure has only been reported by Bhattacharyya [22] as the second most stable isomer.

Pt$_7$ was found to be a side capped double square with an average bond distance of 2.74 Å and triplet spin multiplicity.

The cubic geometry for Pt$_8$ with nonet spin multiplicity and average bond distances of 2.58 Å was found to be most stable, in agreement with Xiao and Wang [19], who obtained bond distances of 2.54 Å.

For Pt$_9$, our results show the one-faced grown cube as the lowest energy isomer with 2.60 Å average value of interatomic distances and septet electronic state, in good agreement with Xiao and Wang [19]. Nie et. al. [21] found these structures for Pt$_8$ and Pt$_9$ as third and second most stable isomers, respectively.

The lowest energy isomer of Pt$_{10}$ cluster is a trigonal bipyramid grown in five faces with an average bond distance of 2.75 Å and septet electronic state. No data for this structure was found in the literature.

For Pt$_{11}$, the most stable structure is a trigonal bipyramid grown in all faces characterized by a septet electronic state and an average value of interatomic distances of 2.62 Å. This structure has not been reported before.

For Pt$_{12}$, our results show a distorted icosahedra as the lowest energy isomer with singlet spin multiplicity and an average value of interatomic distances of 2.77 Å.
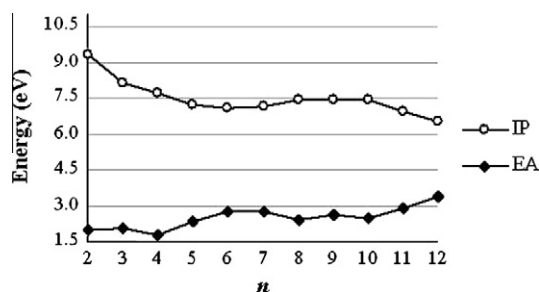


**Fig. 1.** Electron affinity, EA, and ionization potential, IP, as function of cluster size, in eV.

**Table 2**
Ionization potential, IP, electronic affinity, EA, HOMO–LUMO energy gap, $\Delta E$, and global reactivity descriptors, in eV: chemical potential, $\mu$, chemical hardness, $\eta$, and electrophilicity index, $\omega$.

| Cluster | IP | EA | $\Delta E$ | $\mu$ | $\eta$ | $\omega$ |
|---|---|---|---|---|---|---|
| $Pt_2$ | 9.29 | 1.96 | 7.33 | −5.63 | 3.66 | 4.32 |
| $Pt_3$ | 8.17 | 2.05 | 6.12 | −5.11 | 3.06 | 4.26 |
| $Pt_4$ | 7.71 | 1.81 | 5.90 | −4.76 | 2.95 | 3.84 |
| $Pt_5$ | 7.20 | 2.36 | 4.84 | −4.78 | 2.42 | 4.73 |
| $Pt_6$ | 7.08 | 2.79 | 4.30 | −4.93 | 2.15 | 5.67 |
| $Pt_7$ | 7.16 | 2.76 | 4.40 | −4.75 | 2.20 | 4.97 |
| $Pt_8$ | 7.45 | 2.40 | 5.05 | −4.93 | 2.53 | 4.81 |
| $Pt_9$ | 7.47 | 2.59 | 4.88 | −5.03 | 2.44 | 5.19 |
| $Pt_{10}$ | 7.45 | 2.46 | 4.99 | −4.95 | 2.49 | 4.92 |
| $Pt_{11}$ | 6.97 | 2.90 | 4.08 | −4.93 | 2.04 | 5.97 |
| $Pt_{12}$ | 6.50 | 3.35 | 3.15 | −4.93 | 1.58 | 7.70 |

As shown in Table 1, the average bond length, $\langle R \rangle$, increases with cluster size except for $Pt_6$, $Pt_8$ and $Pt_{11}$. This behavior is also accompanied by a decrease in the average coordination number, $\langle CN \rangle$. $\langle CN \rangle$ was obtained by taking the arithmetic mean of the first neighbors' bond lengths at each site.

The magnetic moment per atom is also included in Table 1. Our results indicate that the magnetic moment per atom of the clusters is generally smaller than one and changes according to cluster size in an oscillatory manner.

Furthermore, it is found that the absolute value of the binding energy per atom of Pt clusters increases smoothly as a function of cluster size, indicating that clusters become increasingly stabilized. It is assumed that the cohesive energy in the limit of infinitely large clusters is close to the experimental value of

platinum at bulk level, 5.77 eV/at [39]. It is clear that clusters studied here are still too small to give a reasonable estimation of bulk platinum cohesive energy. Moreover, it is well known that the magnitude of BE/at gives information about the strength of chemical bonds in clusters, thus determining the stability and reactivity of the system might be helpful. In metallic clusters, the increase of this property is due to a high electronic delocalization coming from the atoms' high coordination.

### 3.2. Electronic properties

Calculated ionization potentials (IP) and electron affinities (EA) are shown in Fig. 1 and Table 2. Comparison with the available
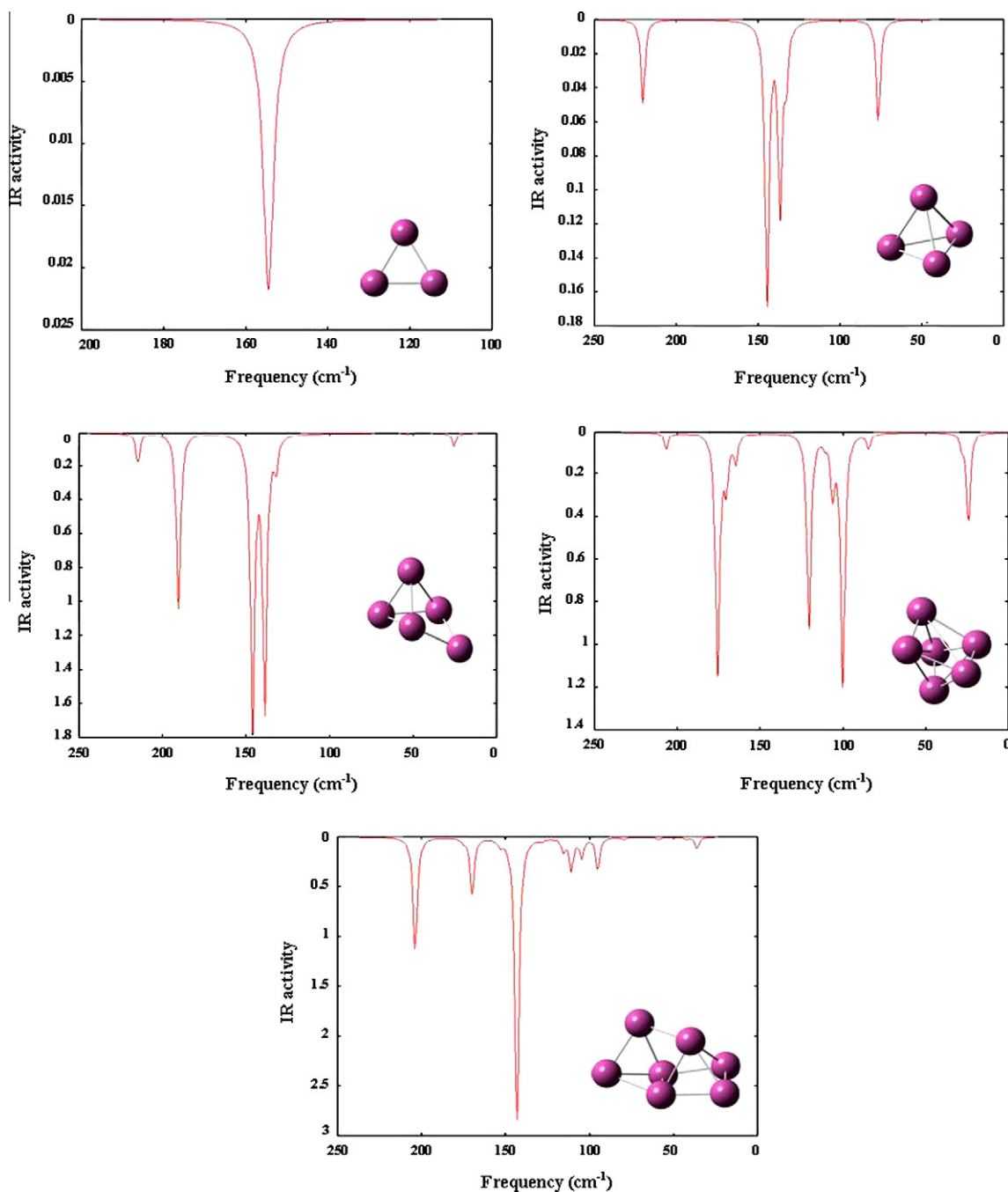


**Fig. 2.** Calculated infrared spectra for $Pt_3$, $Pt_4$, $Pt_5$, $Pt_6$ and $Pt_7$.

experimental data [3,7–9] suggests that experimentally measured IP and EA can be reproduced reasonably well.

Ho and co-authors [7], found that the EA for platinum dimer is 1.898 ± 0.008 eV, in agreement with our calculations. Taylor [3] reported, for the same aggregate, an IP of 8.86 ± 0.02 eV. For the trimer, Ervin and collaborators informed values for the EA of 1.87 ± 0.02 eV [18].

Computations indicate that the IP of small Pt clusters generally decreases with cluster size, while the EA increases with a relatively small variation for larger clusters.

Apart from this, a sensitive quantity to explore chemical reactivity of small Pt clusters is the energy gap; that is, the difference between the highest occupied and the lowest unoccupied molecular orbital energies (HOMO–LUMO). Also, in Table 2, HOMO–LUMO
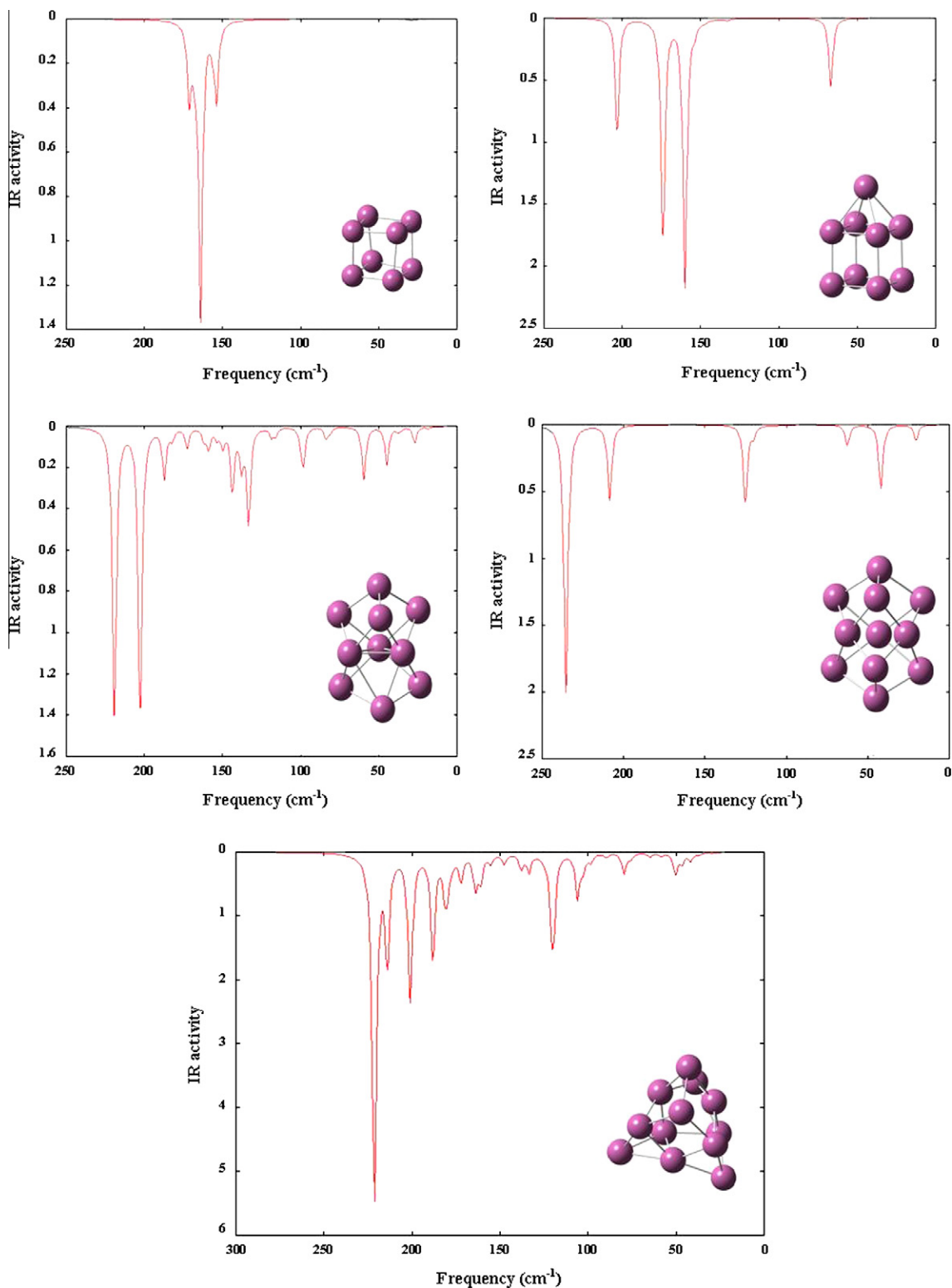


**Fig. 3.** Calculated infrared spectra for $Pt_8$, $Pt_9$, $Pt_{10}$, $Pt_{11}$ and $Pt_{12}$.

gap is shown, calculated as the difference between IP and EA and according to Koopman's theorem [40]. The HOMO–LUMO energy gap shows a decreasing trend with cluster size, being the exceptions $Pt_7$, $Pt_8$ and $Pt_{10}$.

### 3.3. Vibrational spectroscopy

Infrared spectra were computed at the same level of theory as optimizations. Illustrations were made with GaussSum program [41] and are shown in Figs. 2 and 3.

Platinum dimer has been studied in an experimental manner for several groups through diverse spectroscopic techniques [3,7,42]. Our results show that platinum dimer is not active in the IR region. The trimer presents two vibrational modes, 154.53 cm$^{-1}$ and 154.36 cm$^{-1}$ that are assigned to be of symmetric stretches. Due to the closeness of the modes, only one band is seen in the depicted spectrum. Experiments performed by Ervin and co-workers [8] found two frequencies in 105 ± 30 cm$^{-1}$ and 225 ± 30 cm$^{-1}$ for $Pt_3$, considering the lineal structure and assigning this modes to a single band in two different electronic states. In contrast, Lombardi and Davis [42] considered that the two vibrational modes found by Ervin and co-workers [8] are unlikely to be both symmetric stretches and confirm that the stable structure for this system is the triangle found in this work. It can be seen that, despite the minimum numerical differences, our results provide a clear understanding about the vibrational movements of platinum trimer and a good correspondence with experimental data.

Unfortunately, there are no experimental data for the infrared spectra of Pt clusters constituted by a number greater than three atoms, and thus we are not able to compare our theoretical results with other experimental findings. However, we report our results for the whole series, as they can be very useful for future experimental studies.

### 3.4. DFT chemical reactivity descriptors

In this section we focus our attention on the characterization and rationalization of platinum clusters through the use of DFT chemical reactivity descriptors. In Table 2 we display the computed values of the global reactivity descriptors: chemical potential ($\mu$), chemical hardness ($\eta$) and electrophilicity index ($\omega$).

Reactivity is an intrinsic electronic property of the system which indicates its availability for a possible chemical change; global indicators constitute good indexes to the description of the system. The chemical potential measures the electrons' tendency to escape from the system's equilibrium, then, as $\mu$ becomes more negative, it is more difficult to lose an electron but easier to gain one. $\eta$, On the other hand, can be seen as the resistance of a system to transfer its charge, characterizing thus the stability of the system under study. The electrophilicity index, $\omega$, is a measure of the stabilization energy of the system when it is saturated with electrons which come from the external environment.

Our results indicate that $\mu$ presents oscillating values along the series due to the change on the multiplicity of the ground state of the clusters (see Table 2). It is expected that open shell systems present a superior value of $\mu$, because of the easiness of electron transfer. The energetic analysis has only determined two close shell structures as more stable, the equilateral triangle trimer, and $Pt_{12}$. $Pt_3$ shows the second lowest value of the chemical potential in the sequence studied, being $Pt_9$ the one with the greatest value.

$\eta$, Should follow a similar tendency as $\mu$. In fact, it is observed in Table 2 that $Pt_3$ is the second hardest, with a value of 3.06 eV. It might be observed that hardness, in general, decreases as the number of atoms grow. The exception is found in $Pt_7$, $Pt_8$, $Pt_9$ and $Pt_{10}$

clusters. The discrepancy in these results is also observed for IP values, obtaining a peak in Fig. 1 for these clusters.

$\omega$ value determines that platinum dodecamer is the most susceptible of the 12 clusters of receiving electrons from the external environment. The electrophilicity index increases with cluster size and we believe that it is an essential parameter for the subsequent election of a catalyser.

## 4. Conclusions

Geometric, magnetic and electronic features, vibrational frequencies and reactivity descriptors of $Pt_n$ ($n$ = 1–12) were studied in the present work within the framework of the density functional theory. The binding energy per atom was used as a criterion of stability.

The most stable forms found for $Pt_2$, $Pt_3$, $Pt_4$, $Pt_5$, $Pt_6$, $Pt_8$ and $Pt_9$ agree with results reported by other authors. Moreover, the distorted squared pyramid geometry corresponding to $Pt_5$ shows almost the same binding energy as the bipyramid obtained by other authors.

$Pt_7$, $Pt_{10}$, $Pt_{11}$, and $Pt_{12}$ structures have not been reported in the literature before. Data obtained through the vibrational analyses are in line with the results by other authors and contribute to future experimental studies.

Present results indicate that platinum clusters up to twelve atoms tend to increase their reactivity with size. Global reactivity descriptors, chemical potential, chemical hardness and electrophilicity index show that smaller clusters are less reactive.

## References

[1] J. Alonso, Structure and Properties of Atomic Nanoclusters, Imperial College Press, 2005.
[2] G.E. Fryxell, G. Cao (Eds.), Environmental Applications of Nanomaterials: Synthesis, Sorbents and Sensors, Imperial College Press, 2007.
[3] S. Taylor, G.W. Lemire, Y.M. Hamrick, Z. Fu, M.D. Morse, J. Chem. Phys. 89 (1988) 5517–5523.
[4] K. Jansson, R. Scullman, J. Mol. Spectrosc. 61 (1976) 299–312.
[5] S.K. Gupta, B.M. Nappi, K.A. Gingerich, Inorg. Chem. 20 (1981) 966–969.
[6] M. Airola, M. Morse, J. Chem. Phys. 116 (2002) 1313–1317.
[7] J. Ho, M.L. Polak, K.M. Ervin, W.C. Lineberger, J. Chem. Phys. 99 (1993) 8542–8551.
[8] K.M. Ervin, J. Ho, W.C. Lineberger, J. Chem. Phys. 89 (1988) 4514–4521.
[9] W. Eberhardt, P. Fayet, D.M. Cox, Z. Fu, A. Kaldor, R. Sherwood, D. Sondericker, Phys. Rev. Lett. 64 (1990) 780–783.
[10] D.E. Ellis, J. Guo, H.P. Cheng, J.J. Low, Adv. Quantum Chem. 22 (1991) 125.
[11] K. Balasubramanian, J. Chem. Phys. 87 (1987) 6573–6578.
[12] D. Dai, K. Balasubramanian, J. Chem. Phys. 103 (1995) 648–655.
[13] S.H. Yang, D.A. Drabold, J.B. Adams, K. Glassford, J. Phys.: Condens. Matter 9 (1997) L39–L45.
[14] J. Harris, Phys. Rev. B 31 (1985) 1770–1779.
[15] A. Fortunelli, J. Mol. Struct. (Theochem) 493 (1999) 233–240.
[16] Amsterdam Density Functional (ADF), Revision 2.3.0, Theoretical Chemistry, Vrije Universiteit, Amsterdam, 1997.
[17] E. Apra, A. Fortunelli, J. Mol. Struct. (Theochem) 501–502 (2000) 251–259.
[18] D.E. Bernholt, E. Apra, H.A. Frütchtl, M.F. Guest, R.J. Harrison, R.A. Kendall, R.A. Kutteh, X. Long, J.B. Fann, R.J. Littlefield, J. Nieplocha, Int. J. Quantum Chem. Quantum Chem Symp. 29 (1995) 475.
[19] L. Xiao, L. Wang, J. Phys. Chem. A. 108 (2004) 8605–8614.
[20] M.N. Huda, M.K. Niranjan, B.R. Sahu, L. Klinman, Phys. Rev. A 73 (2006) 0532011–0532015.
[21] A. Nie, J. Wu, C. Zhou, Y. Shujuan, C. Luo, R. Forrey, H. Cheng, Int. J. Quantum Chem. 107 (2007) 219–224.
[22] K. Bhattacharyya, C. Majumder, Chem. Phys. Lett. 446 (2007) 374–379.
[23] V. Kumar, Y. Kawazoe, J. Phys. Review B 77 (2008) 2054181-1–2054181-10.
[24] A. Sebetci, Phys. Chem. Chem. Phys. 11 (2009) 921–925.
[25] A. Sebetci, Chem. Phys. 331 (2006) 9–18.

[26] P. Jaque, A. Toro-Labbé, J. Chem. Phys. 117 (2002) 3208–3218.
[27] P.K. Chataraj, G.H. Liu, R.G. Parr, Chem. Phys. Lett. 237 (1995) 171;
P.K. Chataraj, Proc. Indian Natl. Sci. Acad. Part. A 62 (1996) 513;
R.G. Pearson, W.E. Palke, J. Phys. Chem. 96 (1992) 3283.
[28] R.G. Parr, R.G. Pearson, J. Am. Chem. Soc. 105 (1983) 7512–7516.
[29] R.G. Pearson, J. Am. Chem. Soc. 85 (1963) 3533–3539.
[30] R.G. Parr, W. Yang, J. Am. Chem. Soc. 106 (1984) 4049–4050.
[31] Gaussian 03, Revision B.04, M.J. Frisch, G.W. Trucks, H.B. Schlegel, G.E. Scuseria, M.A. Robb, J.R. Cheeseman, J.A. Montgomery, Jr., T. Vreven, K.N. Kudin, J.C. Burant, J.M. Millam, S.S. Iyengar, J. Tomasi, V. Barone, B. Mennucci, M. Cossi, G. Scalmani, N. Rega, G.A. Petersson, H. Nakatsuji, M. Hada, M. Ehara, K. Toyota, R. Fukuda, J. Hasegawa, M. Ishida, T. Nakajima, Y. Honda, O. Kitao, H. Nakai, M. Klene, X. Li, J.E. Knox, H.P. Hratchian, J.B. Cross, C. Adamo, J. Jaramillo, R. Gomperts, R.E. Stratmann, O. Yazyev, A.J. Austin, R. Cammi, C. Pomelli, J.W. Ochterski, P.Y. Ayala, K. Morokuma, G.A. Voth, P. Salvador, J.J. Dannenberg, V.G. Zakrzewski, S. Dapprich, A.D. Daniels, M.C. Strain, O. Farkas, D.K. Malick, A.D. Rabuck, K. aghavachari, J.B. Foresman, J.V. Ortiz, Q. Cui, A.G. Baboul, S. Clifford, J. Cioslowski, B.B. Stefanov, G. Liu, A. Liashenko, P. Piskorz, I. Komaromi, R.L. Martin, D.J. Fox, T. Keith, M.A. Al-Laham, C.Y. Peng, A. Nanayakkara, M. Challacombe, P.M.W. Gill, B. Johnson, W. Chen, M.W. Wong, C. Gonzalez, J.A. Pople, Gaussian, Inc., Pittsburgh PA, 2003.
[32] A.D. Becke, J. Chem. Phys. 98 (1993) 1372–1377.
[33] J.P. Perdew, J.A. Chevary, S.H. Vosko, K.A. Jackson, M.R. Pederson, D.J. Singh, C. Fiolhais, Phys. Rev. B 46 (1992) 6671–6687.
[34] J.P. Perdew, Y. Wang, Phys. Rev. B 45 (1992) 13244–13249.
[35] P.J. Hay, W.R. Wadt, J. Chem. Phys. 82 (1985) 270–283.
[36] E.V. Ortiz, M.B. López, E.A. Castro, J. Phys.: Conf. Ser. 167 (2009) 012021–012025.
[37] R. Parr, R.G. Pearson, J. Am. Chem. Soc. 105 (1983) 7512–7516.
[38] U. Müller, K. Sattler, J. Xhie, N. Venkateswaran, G. Raina, J. Vac, Sci. Technol. B 9 (1991) 829–832.
[39] C. Kittel, Introduction to de Solid State Physcs, seventh ed., J. Wiley & Sons, New York, 1996.
[40] T.A. Koopmans, Physica 104 (1933).
[41] GaussSum 2.1, N.M. O'Boyle, A.L. Tenderholt y, K.M. Langner, J. Comp. Chem. 29 (2008) 839–845.
[42] J. Lombardi, B. Davis, Chem. Rev. 102 (2002) 2431–2460.